2019

# Exercise Training Prevents the Perivascular Adipose Tissue-induced Aortic Dysfunction with Metabolic Syndrome

Evan DeVallance

Kayla W. Branyan

Kent C. Lemaster

Ray Anderson

Kent L. Marshall

*See next page for additional authors*

## Authors

Evan DeVallance, Kayla W. Branyan, Kent C. Lemaster, Ray Anderson, Kent L. Marshall, I. Mark Olfert, David M. Smith, Eric E. Kelly, Randy W. Bryner, Jefferson C. Frisbee, and Paul D. Chantler

Redox Biology 26 (2019) 101285

Contents lists available at ScienceDirect

Redox Biology

journal homepage: www.elsevier.com/locate/redox

# Exercise training prevents the perivascular adipose tissue-induced aortic dysfunction with metabolic syndrome

Evan DeVallance[a], Kayla W. Branyan[a], Kent C. Lemaster[b], Ray Anderson[c], Kent L. Marshall[a], I. Mark Olfert[a], David M. Smith[c], Eric E. Kelley[d], Randy W. Bryner[a], Jefferson C. Frisbee[b,f], Paul D. Chantler[a,e,*]

[a] Division of Exercise Physiology, WVU School of Medicine, Morgantown, WV, USA
[b] Department of Physiology and Pharmacology, Schulich School of Medicine and Dentistry, University of Western Ontario, London, ON, Canada
[c] Department of Biochemistry, WVU School of Medicine, Morgantown, WV, USA
[d] Department of Physiology & Pharmacology, WVU School of Medicine, Morgantown, WV, USA
[e] Department of Neuroscience, WVU School of Medicine, Morgantown, WV, USA
[f] Department of Medical Biophysics, Schulich School of Medicine and Dentistry, University of Western Ontario, London, ON, Canada

ARTICLE INFO

*Keywords:*
Perivascular adipose tissue
Metabolic syndrome
Proteasome
Oxidative stress
Exercise

ABSTRACT

The aim of the study was to determine the effects of exercise training on improving the thoracic perivascular adipose tissue (tPVAT) phenotype (inflammation, oxidative stress, and proteasome function) in metabolic syndrome and its subsequent actions on aortic function.

*Methods:* Lean and obese (model of metabolic syndrome) Zucker rats (n = 8/group) underwent 8-weeks of control conditions or treadmill exercise (70% of max speed, 1 h/day, 5 days/week). At the end of the intervention, the tPVAT was removed and conditioned media was made. The cleaned aorta was attached to a force transducer to assess endothelium-dependent and independent dilation in the presence or absence of tPVAT-conditioned media. tPVAT gene expression, inflammatory /oxidative phenotype, and proteasome function were assessed.

*Results:* The main findings were that Ex induced: (1) a beige-like, anti-inflammatory tPVAT phenotype; (2) a greater abundance of $^{\bullet}NO$ in tPVAT; (3) a reduction in tPVAT oxidant production; and (4) an improved tPVAT proteasome function. Regarding aortic function, endothelium-dependent dilation was greater in exercised lean and obese groups vs. controls ($p < 0.05$). Lean control tPVAT improved aortic relaxation, whereas obese control tPVAT decreased aortic relaxation. In contrast, the obese Ex-tPVAT increased aortic dilation, whereas the lean Ex-tPVAT did not affect aortic dilation.

*Conclusion:* Overall, exercise had the most dramatic impact on the obese tPVAT reflecting a change towards an environment with less oxidant load, less inflammation and improved proteasome function. Such beneficial changes to the tPVAT micro-environment with exercise likely played a significant role in mediating the improvement in aortic function in metabolic syndrome following 8 weeks of exercise.

## 1. Introduction

Metabolic syndrome (MetS) is a cluster of metabolic risk factors (abdominal obesity, elevated blood pressure, impaired glucose tolerance, and dyslipidemia) that is prevalent in approximately 34% of Americans [1]. Individuals with MetS have a three-fold greater risk of death from cardiovascular disease (CVD) compared to healthy individuals [1,2]. As such, unravelling the mechanisms by which MetS is associated with CVD mortality is of critical importance.

Aortic dysfunction is an important mechanism contributing to the elevated incidence of CVD in MetS [3]. We and others have shown that the perivascular adipose tissue surrounding the thoracic aorta (tPVAT) can mediate its function [4,5]. Specifically, in lean rats, the presence of tPVAT improved aortic dilation, whereas in obese rats (Zucker rat; OZR) tPVAT induced vasoconstriction via a tumor necrosis factor alpha (TNFα)-NADPH oxidase (NOX) 2 pathway [4]. We have also shown that the proteasome function of tPVAT plays an important role with the tPVAT mediated aortic dysfunction with obesity [4]. Indeed, an altered redox status of cells can influence proteasome function [6] and, in a vicious cycle, proteasome dysfunction could contribute to the existing

* Corresponding author. One Medical Center Drive, Morgantown, WV, 26505, USA.
*E-mail address:* pchantler@hsc.wvu.edu (P.D. Chantler).

https://doi.org/10.1016/j.redox.2019.101285
Received 28 June 2019; Received in revised form 22 July 2019; Accepted 25 July 2019
Available online 26 July 2019

oxidative and inflammatory environment within the tPVAT [7–9].

It is well established that aerobic exercise training (Ex) is associated with improved cardiovascular health and reduced CVD morbidity/mortality [10–12]. Ex is known to exert its beneficial effects by improving the inflammatory and oxidative environment within the tissue and systemically [13,14]. For example, Ex enhances nitric oxide ($^{\bullet}NO$) bioavailability resulting in vascular homeostasis by modulating vascular tone and decreasing advantageous platelet aggregation [15–18]. Our clinical work has demonstrated that 8-weeks of Ex improves arterial health in patients with MetS [19]. However, the effects of Ex on tPVAT and its subsequent actions on aortic function in MetS is unclear. Further, although Ex has been shown to improve proteasome function in muscle [20] the effect of Ex on proteasome function in tPVAT had not been previously explored. As such, we examined the effects of Ex on tPVAT function and its subsequent regulation of aortic reactivity with MetS. We hypothesized that Ex would prevent tPVAT dysfunction by improving proteasome function and reducing the oxidative and inflammatory environment of the tPVAT; thus, restoring $^{\bullet}NO$ levels. We subsequently hypothesized that such changes would diminish tPVAT-induced impairment of aortic dilation in the context of MetS.

## 2. Methods

### 2.1. Animals

Male lean (LZR, n = 16) and obese (OZR, a valid model of MetS, n = 16) rats were purchased from Envigo Laboratories at 7-9 weeks of age and housed at the West Virginia University Health Science Center (WVUHSC) animal care facility on an approved protocol by the WVUHSC Animal Care and USE Committee (protocol# 1603000971). Animals received standard chow and tap water *ad libitum*. At 16-17 weeks of age, animals were weighed then deeply anesthetized by injection (*i.p.*) of sodium pentobarbital (50 mg/kg). All rats received carotid artery and jugular vein cannulation to measure mean blood pressure and to administer heparin, respectively. Animals were then euthanized via severing of the diaphragm and subsequent removal of the aorta, which was placed in ice cold Krebs Henseleit Buffer (1.18 mM $KH_2PO_4$, 1.2 mM $MgSO_4{\bullet}7H_2O$, 4.7 mM KCl, 25 mM $NaHCO_3$, 118 mM NaCl, 5.5 mM glucose, 26 μM Ethylenediaminetetraacetic acid (EDTA), 2.5 mM $CaCl_2{\bullet}2H_2O$, bubbled with 95% $O_2$). tPVAT was then carefully removed from the aorta under a dissecting microscope, and the aorta was sectioned into 3 mm rings. Aliquots of the tPVAT were collected to assess gene expression, inflammatory mediators, and to create conditioned media to give its role on aortic function.

### 2.2. Exercise training protocol

The rats were randomly assigned into control (LZR-Con and OZR-Con, n = 8/group) or Ex (LZR-Ex and OZR-Ex, n = 8/group) groups. The Ex rats underwent 8 weeks of treadmill running on motor driven treadmill for 5 days/week at 60-70% max speed at 5% grade. During the first week, animals were acclimatized to the treadmill by running for 20 min, then the duration of the running was gradually increased by 10 min/day until 60 min/day was achieved and sustained. A maximum speed test was performed on each animal, and a target running speed was set for 60-70% of that maximum. After acclimatization, the first 15 min of the total 60 min consisted of a gradual increase until target-running speed was reached. Mild electrical stimulus ($\leq$0.3 mA) was used at the rear of the treadmill to discourage rats from stopping. At the end of the 8-week intervention there was a 48-hr wash-out period prior to the terminal surgery.

### 2.3. Gene expression

As we previously described in detail [4], to assess gene expression, 50 mg sections of tPVAT were incubated at 37°C in physiological HEPES buffer (43.7 mM NaCl, 80 mM KCl, 1.17 mM $MgSO_4{\bullet}7H_2O$, 1.6 mM $NaH_2PO_4$, 18 mM $NaHCO_3$, 0.03 mM EDTA, 5.5 mM glucose, 5 mM HEPES). After 1-hr tPVAT was removed and snap frozen in liquid $N_2$. To assess gene expression, tPVAT was homogenized in QIAzol and processed for qPCR using the RNeasy Lipid Tissue MiniKit (Qiagen), QuantiTect reverse transcription kit (Qiagen 205313). Equal concentrations of cDNA were then loaded into the QIAgility (Qiagen), which mixed 20 μL PCR reactions with QuantiTect primer assays and QuantiFast PCR master mix (Qiagen 204056). Relative quantification was carried out by the 2^(-ddCt) method as described previously [4]. The following primers were examined: uncoupling protein 1 (QT00183967), CD4 (QT00181811), CD68 (QT00372204), CD8a (QT00177261), $Gp91^{phox}$ (QT00195300), p47phox (QT00189728), nuclear factor-like 2 (QT00183617), superoxide dismutase -1 (QT00174888) and 2 (QT00185444), glutathione-disulfide reductase (QT01083285), and β-actin was the control gene (QT00193473).

### 2.4. Measurement of oxidative stress

As we previously described in detail [4], dihydroethidium (DHE, Invitrogen D1168) assays were performed on unfixed aortic rings as well as tPVAT sections placed in individual wells of a 96 well plate containing HEPES buffer. Samples were then set in OCT (Fisher Healthcare™), frozen, and then 8 μm sections were mounted on charged slides and imaged with an EVOS fluorescent microscope (Invitrogen EVOS FL Auto Cell Imaging System, Carlsbad, CA RFP light cube ex:531/40em:593/40). Images were taken from 3 randomly selected regions of each sample at 40X magnification. To control for image quality, regions were excluded and new regions selected if the entire sample was not in the same focal plane. Images were analyzed in ImageJ by splitting the color channels generating a grey scale image for the blue, red, and green channels. The red channel image was analyzed for the raw intensity density and the blue channel used to count the number of nuclei in the image. The intensity was divided by the number of nuclei for each image, the 3 images from a sample were averaged then the average of the 3 images were averaged to generate the mean for each animal and represented as mean fluorescent intensity/nuclei. DHE reacts with superoxide ($O_2^{\bullet-}$) to produce a specific product, 2-hydroxyethidium (2-OH-$E^+$), however, we are aware that other DHE-derived products (*e.g.,* E-E dimers and E-HE heterodimers) may contribute to the measured fluorescence as previously reported [21]. To control for $O_2^{\bullet-}$-dependent signal, values were normalized to signal generated in the presence of TEMPOL (i.e., fluorescent signal without tempol/fluorescent signal with tempol). The mean of the LZR control animals was used to calculate relative fold change.

To support results obtained with DHE and further assess oxidative stress via measurement of $H_2O_2$ abundance, tPVAT and treated aortic lysates were analyzed by coumarin boronic acid (CBA, Cayman #14051) assay. CBA probe preparation and protocol were modified from Zielonka et al. [22]. To assess the impact of tPVAT on aortic oxidative stress, donor aortic rings were exposed to tPVAT for 1hr and then aortic segments along with separate tPVAT sample lysates were prepared by 5 rounds of freeze-thaw and passage through a 30-gauge needle. In total, 10 μg of lysates were loaded, in triplicate, into wells of a 384 well black sided clear bottom plate. Subsequently, assay buffer composed of HBSS supplemented with 25 mM HEPES, 1% BSA, 10uM DTPA, 100uM L-NAME, 1 mM Taurine, (L-NAME and Taurine were added to inhibit/sequester peroxynitrite and hypochlorous acid respectively, which could react with the probe) was added and then CBA was added to each well at a final concentration of 0.5 mM. One well from each biological sample received an additional 1 KU/ml bovine liver catalase to act as a negative control. Upon addition of the CBA, plates were placed in a Biotek plate reader preheated to 37°C and read kinetically (every minute for 3 h s) at excitation 350 nm and emission 450 nm. The average rate of fluorescence was determined over the linear portion of the response and then normalized by subtracting out

the rate of fluorescence from the negative control.

### 2.5. Nitric oxide measurement

As we previously described [4], aortic rings were placed in a 96 well plate containing HEPES buffer and 4-amino-5methylamino-2′,7′-difluorofluorescein diacetate (DAF-FM-DA, Invitrogen) supplemented with L-Arginine (100 μM, MP biomedical Inc. 100736), and then stimulated with acetyl-β-methylcholine chloride (methacholine (MCh), $1x10^{-6}$ M, Sigma-Aldrich A2251). The conditioned solution was read in a plate reader excitation/emission at λ = 495/515 nm. Fluorescence was normalized to aortic length while L-NAME treatment was used for validation.

### 2.6. tPVAT cytokine profile

tPVAT, at a ratio of 200mg/1 mL, was incubated for 2h in HEPES buffer to make conditioned media and examined for inflammatory markers (Mesoscale discovery, V-plex K15059D-2) and high molecular weight adiponectin (Mybiosource MBS020496). Additionally, tPVAT homogenates were prepared and examined for inflammatory markers (Mesoscale discovery, K15179C-9), 20S proteasome (Mybiosource MBS730715), and Ubiquitin (Mybiosource MBS039103). All ELISA's were run per manufacturer's instructions as described previously [4]. Additionally, samples were run in standard western blot procedures to analyze the 19S proteasome (Rpt6, ENZO, BML-PW9265-0100) normalized to β-actin (cell signaling #49705).

### 2.7. tPVAT tissue function

As we previously described [4], tPVAT homogenates were used to examine total (CuZn and MnSOD) superoxide dismutase (SOD) activity (Sigma-Aldrich 19160-1 KT-F), and proteasome function assays: LLVY-AMC (ENZO BML-P802-0005), nLPnLD-AMC (Bachem I-1850.0005), and RLR-AMC (Boston Biochem S-290) run per manufacturer's instructions. Additionally, to directly test 19S mediated 26S proteasome function, tPVAT homogenates were run in $Ub_4$ (lin)-GFP-35 (0.08 μg/reaction) degradation assays carried out in 50 μl reactions using 96-half-well black plates (Corning) at 37°C. GFP fluorescence was measured every 60 s for 4 h (ex/em:485/528) on BioTek plate reader (BioTek Synergy HT, Winooski, VT). The $Ub_4$ (lin)-GFP-35 substrate, generously supplied by Dr. David M. Smith, was generated as described by Martinez-Fonts and Matouschek [23]. V-max for each assay was determined from 30 points on the linear portion of the kinetic read and normalized to V-max in the presence of the 20S inhibitor MG132 to account for background.

### 2.8. Aortic reactivity

As we previously described [4], 3 mm thoracic aortic rings (cleaned of surrounding tissue) were rinsed in physiological salt solution and mounted in a myobath chamber between a fixed point and a force transducer (World Precision Instruments) pre-stretched, and allowed to equilibrate for 1-hr in Krebs Henseleit Buffer aerated with 95%$O_2$ and 5%$CO_2$ at 37°C. After equilibration, aortic baseline tension was adjusted to 1 g and vessel viability was checked with 50 mM of KCl and rings not generating a rapid response were excluded from the study. To test endothelial dependent dilation (EDD), aortic rings were pre-constricted with phenylephrine PE, $1x10^{-7}$ M Sigma-Aldrich P6126) and a stable tension was reached and recorded followed by increasing doses of MCh ($1x10^{-9}$ M-$1x10^{-5}$ M). Dilation was calculated as %relaxation for each dose of MCh from the following equation:

$$\%\text{relaxation} = \left(\frac{Z - x}{Z - y}\right) \times 100,$$

where z = tension after PE $1X10^{-7}$M, x = tension following a given does of MCh, and y = baseline tension.

Following the MCh curve, the system was washed again and allowed to return to baseline. To test the effect of tPVAT on EDD, tPVAT exudate was snap frozen and used in crossover experiments. Exudate was added to the bath and rings incubated for 30 min. To directly test the role of proteasome function in lean tPVAT on tPVAT mediated aortic dilation; we incubated the tPVAT with MG132, a potent cell-permeable proteasome inhibitor. Following the incubation, relaxation curves was performed as described above. Pilot studies demonstrated no difference in EDD between exudate vs. tPVAT tissue incubation.

### 2.9. Statistics

We have previously shown that in LZR that tPVAT improved aortic dilation by 5%, and that OZR tPVAT reduced aortic function by 10% [4]. As such, we performed a power analysis using PASS software with a repeated measures analysis. The analysis was powered off the interaction term between tPVAT and Ex group to establish a 10 ± 5% (SD) improvement in aortic dilation with tPVAT in the OZR Ex group, for an effect of 1.66. Assuming 0.5 correlation between time points and alpha set to 0.05, total of 4 rats per group was needed to detect the interaction effect with 0.97 power. However, we doubled that sample size to account for potential experimental issues. All data are represented as mean ± standard deviation. All experiments were run in duplicate and the average of the reads used as the mean for each animal. Data analysis and graphing were conducted using GraphPad Prism 6 software (GraphPad Software, Inc.) and $p \leq 0.05$ was set for statistical significance. Comparisons between groups were conducted using a one-way ANOVA, and a repeated measure ANOVA for aortic reactivity with Tukey post-hoc test used to determine differences between groups.

## 3. Results

Animal Characteristics: Rat phenotypic characteristics are presented in Table 1. As expected, by study design, the OZR (controls and Ex) demonstrated greater body mass, MAP, glucose levels, and lipid abundance when compared to LZR (controls and Ex). Crucial to data analysis and conclusions from our experimental data, no differences in body mass and MAP were noted within the LZR and OZR groups, except for triglycerides and total cholesterol, which were lower in OZR-Ex compared to OZR control.

### 3.1. tPVAT regulation of aortic function

#### 3.1.1. Analysis of aortic oxidant state

In aortic rings, no differences were found in global aortic SOD activity between the LZR-Ex and OZR-Ex groups vs. their respective controls (Fig. 1A). However, a lower SOD activity was noted in both OZR-controls and Ex rats vs. LZR groups ($p < 0.05$). In contrast, aortic $O_2^{\bullet-}$ production, which was higher in OZR vs. LZR-controls, was lower in OZR-Ex vs. OZR-controls ($p < 0.01$, Fig.1B and Fig. S1). Incubation of the OZR-control aorta with OZR-control tPVAT increased aortic $O_2^{\bullet-}$

**Table 1**
Rat phenotype.

| | LZR | | OZR | |
|---|---|---|---|---|
| | Control | Exercise | Control | Exercise |
| Body Mass (g) | 436 ± 18 | 370 ± 11* | 606 ± 10* | 627 ± 19* |
| MAP (mmHg) | 107 ± 2 | 114 ± 2 | 133 ± 5* | 134 ± 6* |
| Glucose (mg/dl) | 98 ± 6 | 101 ± 8 | 184 ± 12* | 154 ± 12* |
| TG (mg/dl) | 25 ± 3 | 31 ± 3 | 124 ± 8* | 82 ± 15*# |

Data represented as Mean ± SD. *$p < 0.05$ vs. LZR-Con; #$p < 0.05$ vs. OZR-Con; MAP, mean arterial pressure; TG, triglyceride.

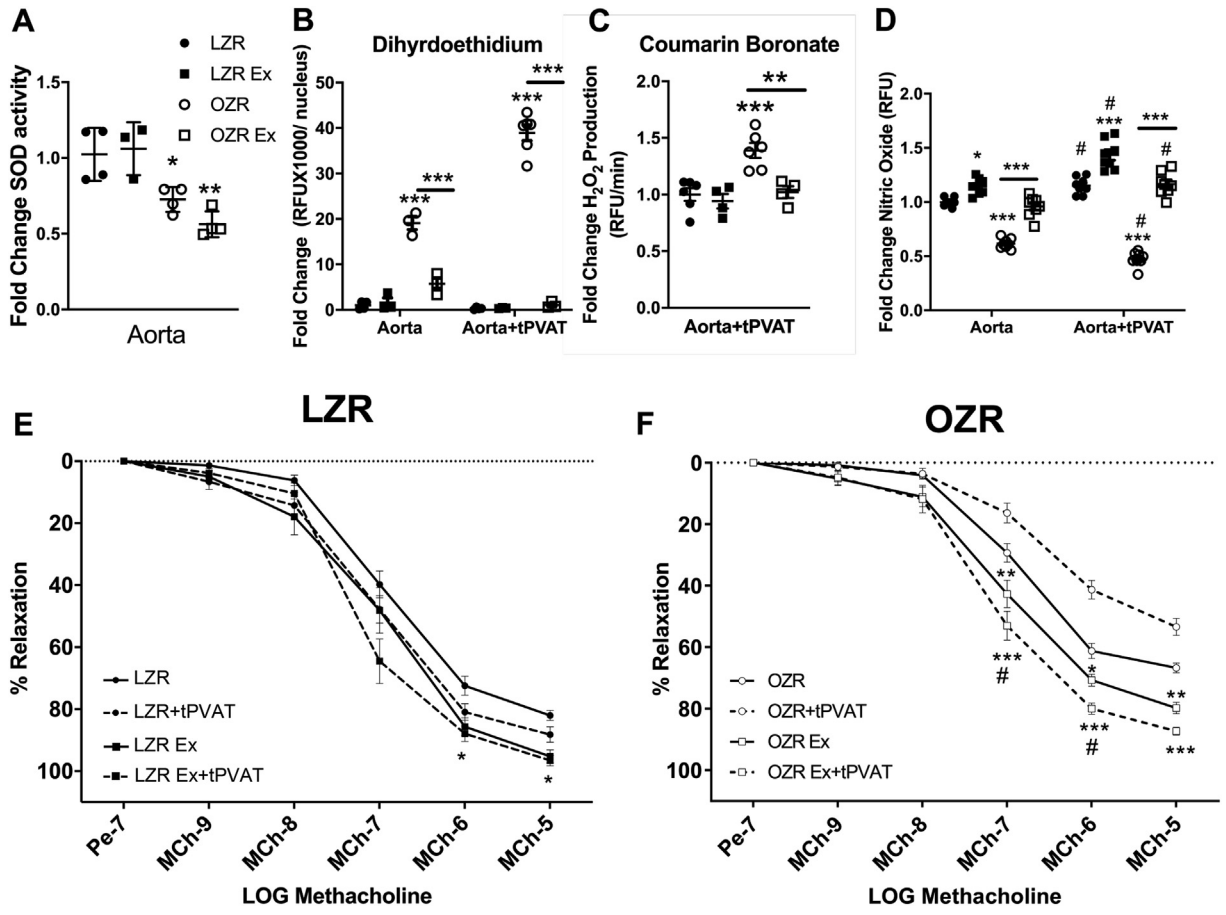


**Fig. 1. Effect of Exercise on tPVAT Mediated Aortic Function**. Aortic total superoxide dismutase (SOD) activity (**A**, n = 3–5), oxidative load measured by dihydroethidium (**B**) and coumarin boronate (**C**) with and without tPVAT incubation (n = 5–8). Aortic nitric oxide ($^{\bullet}$NO) production in the presence or absence of tPVAT (**D**, n = 8) was measured by 4-Amino-5-methylamino-2′,7′-difluorofluorescein diacetate (DAF-FM). Aortic relaxation to methacholine (MCh) in the presence or absence of tPVAT conditioned media in LZR (**E**, n = 8) and OZR (**F**, n = 8). Data are represented as Mean ± SD. For panels **A-D**, *p < 0.05, **p < 0.01, ***p < 0.001 compared to LZR or between groups connected by a bar. For panels **E & F**, *p < 0.05, **p < 0.01, ***p < 0.001 compared to LZR or OZR control without tPVAT, #p < 0.05 vs. LZR or OZR Ex without tPVAT.

production almost 20-fold ($p < 0.001$). Whereas, incubation of the OZR-Ex aorta with OZR-Ex tPVAT reduced aortic oxidative load to minimal levels compared to OZR-Ex aorta without tPVAT incubation ($p < 0.01$, Fig.1B and Fig. S3). Aortic $O_2^{\bullet-}$ production did not differ between LZR-control and LZR-Ex in the presence or absence of its tPVAT (Fig.1B, Figs. S1 and S2). To verify the role of tPVAT in the induction of aortic oxidative stress by assessing $H_2O_2$ abundance, aortic lysates from healthy donors, following their exposure to tPVAT from the intervention groups, were exposed to CBA. Rate of $H_2O_2$ production was significantly increased in aortic lysates exposed to OZR tPVAT compared to LZR tPVAT which was abolished in the aortic lysates exposed to OZR-Ex tPVAT (Fig. 1C).

### 3.1.2. Aortic reactivity

Aortic EDD was greater ($p < 0.05$) in LZR-Ex and OZR-Ex groups (without tPVAT) compared to controls (Fig. 1 E&F). This was likely due to a higher aortic $^{\bullet}$NO production in the Ex groups, as reflected by a greater DAF-FM signal in the LZR-Ex and OZR-Ex groups vs. their controls ($p < 0.05$). In addition, the DAF-FM signal was further increased in the presence of tPVAT from LZR-Ex and OZR-Ex groups (Fig. 1D). Aortic EDD in the OZR-Ex groups was increased in the presence of their own tPVAT, whereas in the OZR control group, the control OZR tPVAT mediated aortic constriction rather than dilation (Fig. 1F). With the LZR-Ex aorta, LZR-Ex tPVAT did not affect EDD, however, in the LZR control group, aortic EDD was further improved with LZR control tPVAT (Fig. 1E).

### 3.1.3. tPVAT environment

Uncoupling protein-1 (UPC-1) expression was higher ($p < 0.01$, Fig. 2A) in the LZR and OZR-Ex groups vs. their respective controls. Further, the OZR-Ex tPVAT had a lower expression of immuno-attractant cytokines, and immune cell specific markers vs. the OZR-control tPVAT (Fig. 2B). Additionally, the production of $^{\bullet}$NO was lower in OZR-control tPVAT compared to LZR-control tPVAT, and higher in OZR-Ex tPVAT vs. OZR-control tPVAT ($p < 0.05$, Fig. 2C).

### 3.1.4. Oxidative stress

No difference was noted in tPVAT $O_2^{\bullet-}$ or $H_2O_2$ production between LZR-controls and LZR-Ex. However, the elevated $O_2^{\bullet-}$ and $H_2O_2$ production from tPVAT in OZR-controls was not evident in OZR-Ex group (Fig. 2 D&E). The lower oxidative signal in OZR-Ex tPVAT may partially be explained by a higher total SOD activity ($p < 0.05$, Fig. 2F), and a lower gene expression of GP91 (the catalytic subunit of NOX2) ($p < 0.05$, Fig. 2G) in the tPVAT OZR-Ex vs. OZR-controls. However, no differences in tPVAT gene expression was noted between the OZR-Ex and OZR-control groups for the NOX2 regulatory subunit, p47phox. Expression of other redox factors, SOD 1 and 2, Nrf2, and GSR were higher in the OZR-Ex vs. OZR-control group (data not shown).

### 3.1.5. Proteasome function

As the oxidative load/redox status of cells is known to impact the ubiquitin-proteasome-system, we next examined tPVAT proteasome function. The LZR-Ex group had a greater activity of the chymotrypsin-

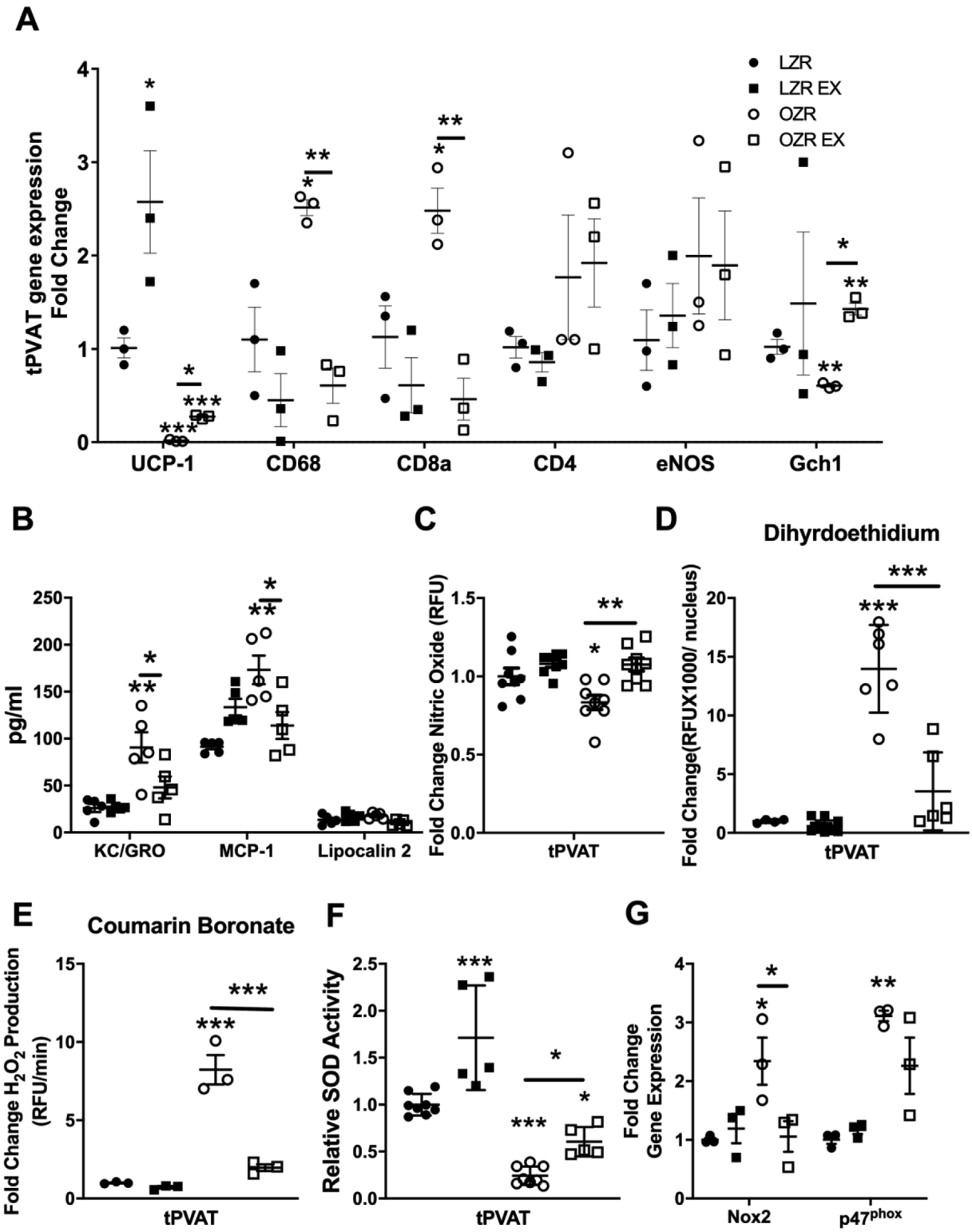


**Fig. 2. tPVAT Environment**. qRT-PCR was used to assess tPVAT relative gene expression of phenotype indicators and immune cell markers (**A**, n = 3), while immune-attracting cytokines (keratinocyte chemoattractant (KC)/human growth-regulated. oncogene (GRO), monocyte chemoattractant protein-1 (MCP-1), and lipocalin 1 were measured in tPVAT conditioned media (**B**, n = 5). tPVAT production of $^{\bullet}NO$ measured by fluorescent DAF-FM (**C**, n = 8), oxidative load measured by dihydroethidium (**D**, n = 5) and coumarin boronate (**E**, n = 5), and relative SOD activity (**F**, n = 4–6). Finally, gene expression of two subunits of the NOX2 enzyme ($Gp91^{phox}$, p47phox) (**G**, n = 3). Data are represented as Mean ± SD. *p < 0.05, **p < 0.01, ***p < 0.001 compared to LZR or between groups connected by a bar. UCP-1, uncoupling protein-1; CD, cluster of differentiation; eNOS, endothelial nitric oxide synthase; Gch-1, GTP cyclohydrolase; SOD, superoxide dismutase; NOX2, NADPH oxidase 2 catalytic subunit (GP91); p47phox, NADPH oxidase 2 intracellular regulatory subunit.

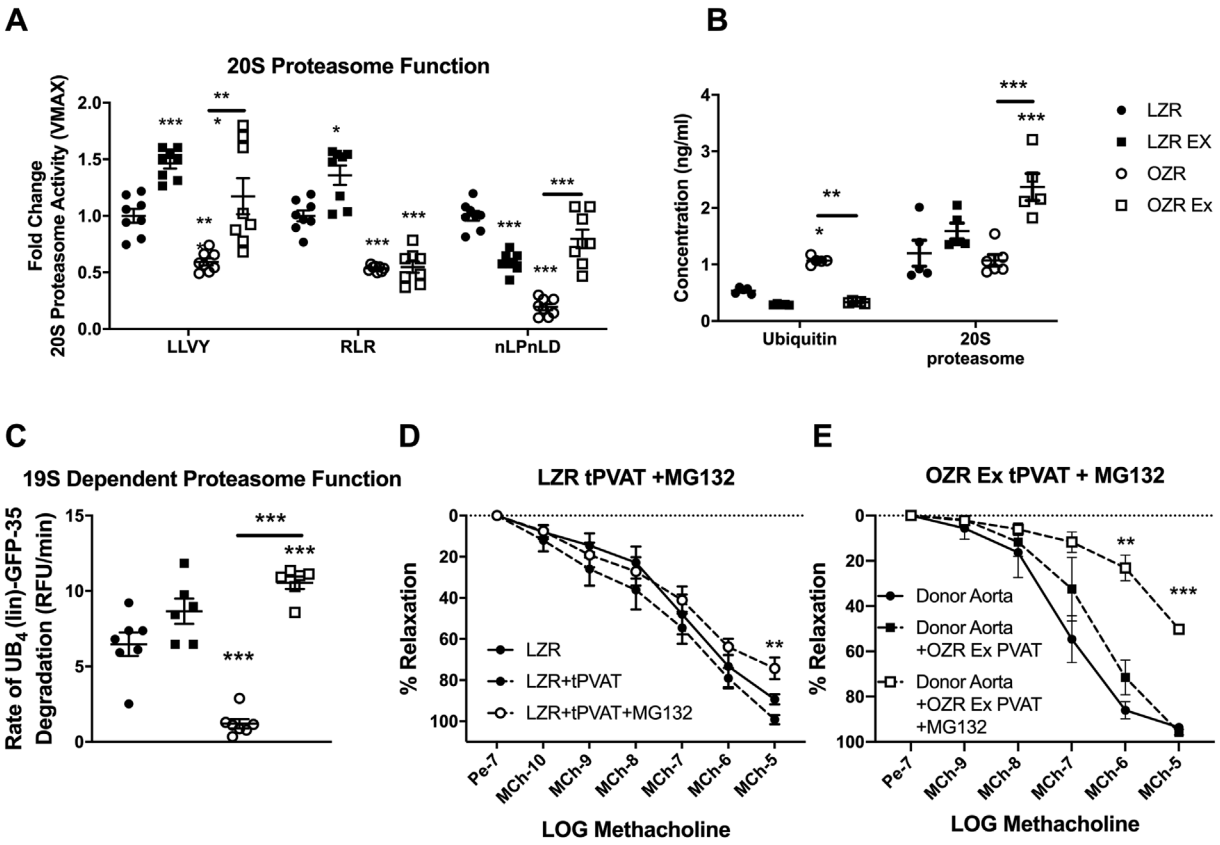


**Fig. 3. Exercise Enhancement of Proteasome Function**. tPVAT samples were measure for proteasome protease activity at all three 20S active sites (**A**, n = 6–8); LLVY (chymotrypsin-like), RLR (trypsin-like) and nLPnLD (caspase-like site). tPVAT samples were analyzed for levels of ubiquitin and the 20S proteasome beta-subunit (**B**, n = 5). Ubiquitin-dependent 26S proteasome substrate degradation was measured in tPVAT samples by a linier ubiquitin chain-GFP substrate (**C**, n = 6–8). Aortic relaxation was assessed in LZR aortic rings incubated with LZR tPVAT pre-treated with the proteasome inhibitor MG132 (**D**, n = 4). Effects of proteasome inhibition in OZR Ex tPVAT on endothelial dependent dilation of healthy (donor) aortas (**E**, n = 4). Data are represented as Mean ± SD. For panels **A-C**, *p < 0.05, **p < 0.01, ***p < 0.001 compared to LZR or between groups connected by a bar. For panels **D** and **E**, **p < 0.01 compared to LZR control tPVAT or OZR Ex tPVAT with MG132.

like active site and trypsin-like active site ($p < 0.05$). Whereas, the tPVAT from the OZR-Ex group had greater activity of the chymotrypsin-like active site and peptidylglutamyl-peptide hydrolyzing active site (Fig. 3A) compared to OZR-control ($p < 0.05$). Additionally, a greater tPVAT expression of the 20S catalytic core was noted in the OZR-Ex ($p < 0.05$) but not in the LZR-Ex group (Fig. 3B). The improved 20S core activity was accompanied by a lower expression of ubiquitin in both LZR-Ex and OZR-Ex vs. their respective controls ($p < 0.05$, Fig. 3B).

Ubiquitin degradation is dependent upon the 19S regulatory cap of the proteasome, therefore we assessed 19S-dependent degradation. The 19S dependent degradation rate of fluorescent ubiquitin was greater in the LZR-Ex and OZR-Ex groups compared to their respective controls ($p < 0.05$, Fig. 3C). To test a direct effect of proteasome function on tPVAT mediated aortic relaxation, LZR tPVAT and OZR-Ex tPVAT were pretreated with 100 μM of MG132. Inhibition of proteasome function in LZR tPVAT and OZR-Ex tPVAT resulted in a tPVAT mediated blunting of aortic EDD (Fig. 3 D&E). These data highlight the beneficial effects of Ex on tPVAT phenotype and subsequent function and suggest improved tPVAT proteasome function as mechanism of Ex adaptation.

### 3.1.6. tPVAT cytokine production

Both oxidative stress and ubiquitinated proteins can stimulate pro-inflammatory cytokines production. In tPVAT, LZR-Ex had similar anti- and pro-inflammatory cytokine profile compared to LZR-controls (Fig. 4). However, a greater abundance of HMW adiponectin was noted in the LZR-Ex tPVAT vs. LZR-control ($p < 0.05$, Fig. 4A). OZR-Ex tPVAT had 30-120% greater ($p < 0.05$) levels of IL-4, IL-5, IL-10, IL-13 and HMW adiponectin compared to OZR-controls (Fig. 4A). Interestingly, the tPVAT in the OZR-Ex group had a 75% and 25% less ($p < 0.05$) TNFα and TSP-1 concentration compared to OZR controls, respectively, with no differences in tPVAT release of IFN-γ or IL-1β (Fig. 4B). These data suggest Ex prevented the increased release of TNFα from tPVAT associated with MetS, and increased IL-10 and restored HMW adiponectin.

### 3.1.7. tPVAT crossover experiments

With both tPVAT dependent and independent effects on aortic function improved following Ex, we examined if the aortic EDD in the OZR-Ex was protected from the detrimental effects of tPVAT from OZR controls. Indeed, incubation of the OZR-Ex aorta with non-Ex OZR tPVAT blunted the aortic EDD compared to OZR-Ex aorta without tPVAT ($p < 0.01$, Fig. 5). Interestingly, incubation of the OZR-Ex aorta with LZR-control tPVAT improved aortic EDD to relatively the same extent as when OZR-Ex aorta was incubated with its own tPVAT (Fig. 5).

## 4. Discussion

Here we provide novel data suggesting that Ex prevented tPVAT dysfunction in MetS with a corresponding improvement in tPVAT-mediated aortic function. Specifically, we have shown that 8-weeks of Ex in OZR significantly improved tPVAT $^{\bullet}$NO bioavailability, reduced oxidative stress levels, increased proteasome function, and reduced

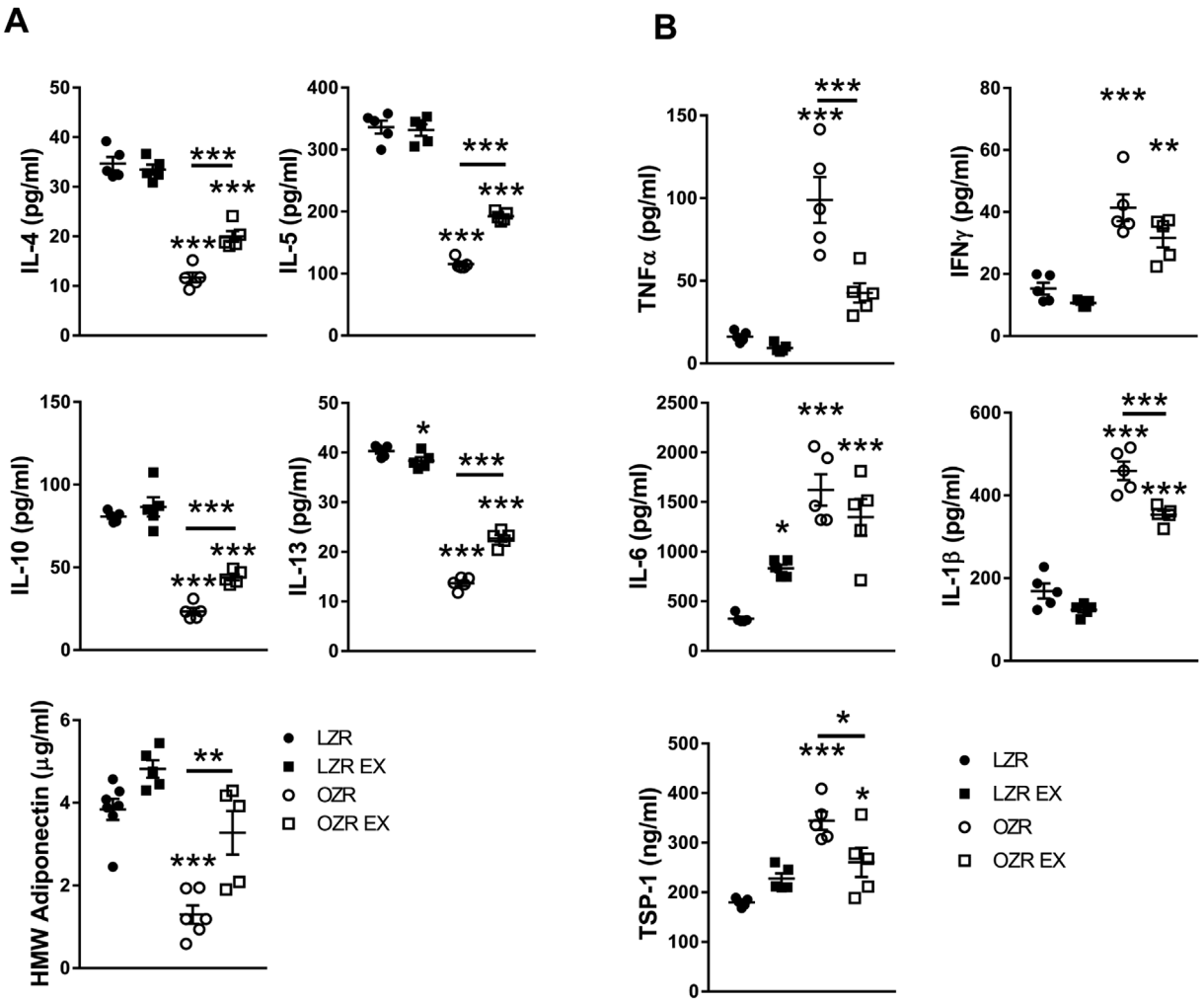


**Fig. 4. tPVAT Cytokine Profile**. tPVAT conditioned media was assessed by multi-plex array for anti-inflammatory (**A**, n = 5), and pro- inflammatory cytokine levels (**B**, n = 5). Data are represented as Mean ± SD. *p < 0.05, **p < 0.01, ***p < 0.001 compared to LZR or between groups connected by a bar. IL, interleukin; HMW adiponectin, high molecular weight adiponectin; TNFα, tumor necrosis factor alpha; IFN-γ, interferon gamma; TSP-1, thrombospondin 1.

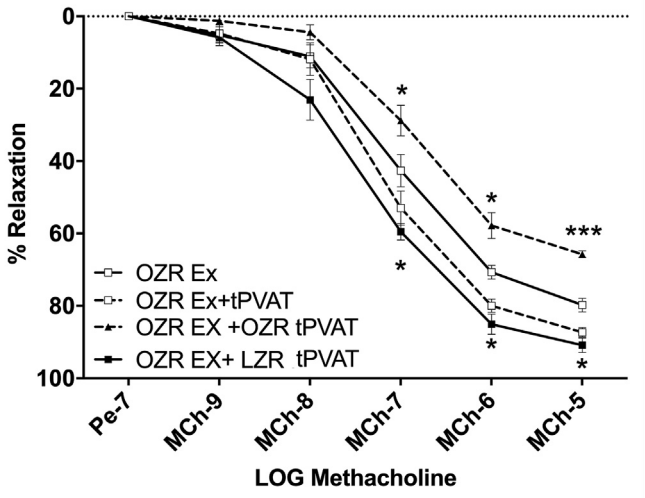


**Fig. 5. Exercise Does Not Protect the Aorta Against tPVAT Derived TNFα Mediated Impairment**. EDD of OZR-Ex aortas after incubation with either OZR Ex-tPVAT (n = 5) or with a crossover treatment with OZR control tPVAT (n = 5), or LZR control tPVAT (n = 5). Data are represented as Mean ± SD. *p < 0.05, ***p < 0.001 compared to OZR-Ex aorta.

inflammatory cytokine profile. Additionally, our data suggested that the improved tPVAT phenotype was essential for the improved aortic function following Ex.

### 4.1. Effect of exercise on tPVAT

#### 4.1.1. tPVAT phenotype

White adipose tissue phenotypes are associated with increased oxidative stress and inflammation [24–26], and a loss of the brown-like phenotype marker (uncoupling protein-1) [26]. Concomitantly, dysregulation of $^{\cdot}$NO and endothelial $^{\cdot}$NO synthase uncoupling are implicated in adipose dysfunction [27] and a loss in the brown/beige phenotype [28,29]. Our data suggested that Ex limited the shift in the tPVAT phenotype associated with MetS, reflected by reduced oxidative load, inflammation, and immune populations and a greater Gch1 expression in the OZR-Ex tPVAT. The increased Gch1 expression is important given that it provides instructions for generating GTP cyclohydrolase 1, which is involved in the production of tetrahydrobiopterin. Importantly, tetrahydrobiopterin is an essential cofactor for $^{\cdot}$NO generation via endothelial $^{\cdot}$NO synthase. Indeed, our data showed an increase tPVAT $^{\cdot}$NO production with Ex. The retention of the brown adipose phenotype in OZR-Ex, in turn, may support a more reductive/anti-oxidant microenvironment in tPVAT [25].

The direct mechanisms driving the promotion of $^{\cdot}$NO in tPVAT with Ex is unknown. However, it has been suggested the myokines from the

exercising muscle [28] and autocrine signaling of adiponectin, which was greater in OZR-Ex, can promote adipose $^{\bullet}$NO signaling and browning of adipose tissue [30]. Specifically, metabolic products (lactate) along with myokines, irisin and meteorin-like 1 induce adipocyte browning (see detailed review [31]), which could have contributed to the findings in the current study. However, a role for these factors in restoring a healthy tPVAT phenotype or proteasome function in obesity have not been established and warrants future investigation. Alternatively, sympathetic nervous system input has been implicated in the brown adipose phenotype and Ex is known to increase sympathetic innervation in both brown [32] and subcutaneous white adipose tissue [33]. Thus, it is possible that similar mechanisms contributed to the browning of the tPVAT in the OZR-Ex group. Detailed mechanistic studies utilizing genetic manipulations are needed to determine the essential factors mediating tPVAT $^{\bullet}$NO, proteasome function, and the brown-like phenotype following Ex training.

Our previous work demonstrated the NOX2 enzyme was a major source of oxidant production in OZR tPVAT [4]. In the present study, Ex mitigated the expression of NOX2, which was accompanied by a significant reduction in oxidative stress measured by DHE and CBA in the OZR-Ex group. It is likely that alterations in immune cell number [34] and function [35,36] along with increased SOD activity contributed to this response. This idea is partial supported by our data, which showed reduced gene expression of pro-inflammatory immune cell markers.

#### 4.1.2. Proteasome Function

The greater oxidative load in OZR tPVAT may contribute to, and be exacerbated by, proteasome dysfunction. It has been suggested that more robust oxidative environments may cause the 19S cap to dissociate from the 20S core reducing the ability to recognize and degrade ubiquitinated proteins [6]. Proteasome dysfunction would be expected to mediate a buildup of ubiquitinated proteins, which has been linked to increased inflammatory cytokines, oxidants, and adipose dysfunction, all key pathologies in MetS [7–9]. Ex has been shown to improve proteasome function in muscle [20] but the effect of Ex on proteasome function in tPVAT had not been previously explored. We showed that Ex improved both 20S and 26S proteasome activity, and the concomitant reduction in ubiquitin was also observed. The increased activity of the 26S proteasome was likely via the upregulation of 19S cap subunits, as the 19S regulatory particle is required for recognition of ubiquitinated proteins (Fig. 3) [37] and 20S gate opening [38], which facilitates protein degradation. Taken together, Ex resulted in a higher concentration of the 19S regulatory cap (both in LZR and OZR) and the 20S core (OZR), which comprise the 26S proteasome. The greater proteasome function likely improved the recognition and breakdown of ubiquitinated proteins, supported by the $Ub_4$ (lin)-GFP-35 substrate assay results (Fig. 3), and the reduction in the inflammatory signaling in MetS. The importance of proteasome function in the tPVAT was further supported by our data showing inhibition of the proteasome (with MG132) in LZR tPVAT and OZR-Ex tPVAT blunted the actions of tPVAT on aortic EDD.

#### 4.1.2. tPVAT Immune cells and Cytokines

In addition to adipocytes, PVAT also includes a stroma vascular fraction, which is a heterogeneous population of cells including immune cells (macrophages, B-and T-lymphocytes) [39]. Immune cells that infiltrate dysfunctional adipose tissue are thought to be key drivers of adipose tissue inflammation. Indeed, with obesity, the adipose tissue inflammation is accompanied by increased infiltration [40] and phenotypic switching [41] of macrophages to a proinflammatory activation profile. The proinflammatory macrophage phenotype (known as M1) produce inflammatory cytokines such as TNFα and IL-6. In addition, evidence suggests that T cells also play an essential role in the development of adipose tissue inflammation [42,43]. $CD8^+$ T cells produce monocyte chemoattractant proteins (MCPs) and macrophage inflammatory proteins, which modulate the infiltration of macrophages in adipose tissue [44]. Further, cytotoxic $CD8^+$ T cells secrete TNFα, IL-2, IFN-γ, whereas treatment of obese mice with CD8-specific antibodies was shown to attenuate M1 macrophage infiltration and adipose tissue inflammation [45]. Our data also showed that in the OZR tPVAT, the mRNA expression of these pro-inflammatory markers were elevated compared to lean controls. In contrast, the OZR-Ex group showed a reduced expression of these inflammatory cell markers (CD68, and CD8) compared to OZR control, which corresponded with a lower concentration of TNFα, IFN-γ, IL-6, and IL-1β. These data suggest that Ex reduced tPVAT inflammation, in part, by preventing the infiltration of T-cells and macrophages. Previous studies have reported that even a single exercise bout, albeit in epididymal fat (white adipose tissue), can induce a phenotypic switch in macrophage populations (i.e., from M1 to M2), and reduce TNFα, IL-1β and MCP-1 mRNA levels [36]. Similarly, Ex for 16 weeks in mice feed a high fat diet, reduced CD11c + inflammatory macrophages and $CD8^+$ T cells in epididymal adipose tissue, which was accompanied by a lower mRNA expression of TNFα compared to the obese mice without Ex [46]. These anti-inflammatory Ex adaptations likely played an important role in preserving/restoring the beneficial relationship between tPVAT and aortic function.

The OZR-Ex group had two lower inflammatory cytokine signaling pathways compared to OZR-Con. First, ubiquitin products [7,8], and second oxidative load [47]. tPVAT from OZR-Ex had a lower production of TNFα, and higher production of IL-10 and HMW adiponectin vs. OZR-controls. IL-10 is a known inhibitor of TNFα [48] and $O_2^{\bullet-}$ [49]. The reduced production of TNFα and immune cells in OZR-Ex tPVAT likely had 3 important actions on the autocrine signaling of tPVAT. First, lower TNFα levels removes autocrine activation of oxidative stress from tPVAT, which can subsequently: a) decrease the oxidative dissociation of the 19S from the proteasome thereby imp roving proteasome function; b) decrease the sequestration of $^{\bullet}$NO; and c) decrease inflammation-controlled gene expression. Second, flipping the TNFα-adiponectin balance towards adiponectin would promote the autocrine activation of enhanced $^{\bullet}$NO abundance and phenotype maintenance [50]. Third, lower TNFα levels could downregulate TSP-1 (Fig. 3). Indeed, increased TSP-1 can inhibit $^{\bullet}$NO production [51], mediate immune cell infiltration [52], and negatively regulate microvascular density [42,53] all of which may negatively impact tPVAT phenotype and function. These actions would have important implications on the tPVAT mediated function of the aorta [50,54].

### 4.2. Role of tPVAT on aortic function

#### 4.2.1. Aortic function

It is well known that Ex can improve arterial health, in particular, the hemodynamic forces (i.e., shear stress) exerted during exercise on the arterial wall plays a key role in regulating arterial function and structure [55]. This shear stress response, sensed by endothelial cells, can affect multiple signaling pathways (integrins, ion channels, G-protein-coupled receptors, and receptor tyrosine kinases), which in turn lead to the establishment of an adaptive response (see detailed reviews for further information [56,57]). It is also plausible that the hemodynamic forces exerted on the arterial wall and smooth muscle, which can improve the oxidative (improved efficiency of the antioxidant system and reduced superoxides) and inflammatory environment of the vasculature, could have exerted beneficial effects on tPVAT. Indeed, our study data confirmed the classic vascular adaptation following Ex where by aortic $O_2^{\bullet-}$ was less and $^{\bullet}$NO abundance greater in OZR-Ex, respectively, which improved aortic EDD (independent of changes in body weight or MAP). Surprisingly, we found no change in SOD activity in either Ex group. However this may be due to differing effects of Ex on the various isoforms of SOD [18], or due to the time in which the sample was analyzed [58]. Despite the important of exercise induced shear stress on improving arterial function, it has been shown that in arteries with a similar structure and exposed to similar hemodynamic

forces display distinct arterial phenotypes [59]. Such data would suggest that other local factors besides shear stress influence the regulation of arterial function, and that tPVAT may be involved [60].

#### 4.2.2. tPVAT mediated aortic function

Although the mechanism(s) by which Ex improved tPVAT health, and the subsequent actions on the aorta, are not fully known they may be concomitantly mediated by autocrine, endocrine, and mechanical signaling. In the current study, improved tPVAT mediated aortic EDD was likely the result of increased $^{\bullet}NO$ bioavailability and reduced activation of aortic $O_2^{\bullet-}$ an/or $H_2O_2$ in OZR-Ex tPVAT. We have previously shown that tPVAT-induced aortic $O_2^{\bullet-}$ was primarily mediated by TNFα in OZR [4]. Thus, diminished TNFα release from OZR-Ex tPVAT is a likely explanation for the reduction of tPVAT-induced aortic $O_2^{\bullet-}$ and $H_2O_2$ observed in the OZR Ex group. Further, increased IL-10 levels noted in the OZR-Ex tPVAT may have limited the activation of oxidative enzymes in the aorta, specifically IL-10 can inhibit NOX-derived $O_2^{\bullet-}$ [49], a significant contributor to aortic $O_2^{\bullet-}$ production [4,61]. The $O_2^{\bullet-}$ scavenging of $^{\bullet}NO$ is a well-known mediator of endothelial dysfunction, suggesting the significant reduction in tPVAT-induced aortic $O_2^{\bullet-}$ production, contributed to the higher levels of $^{\bullet}NO$ found in OZR-Ex aorta.

In addition, to the Ex-induced changes in TNFα, the increased secretion of HMW adiponectin identified in OZR-Ex tPVAT may have contributed to the improved aortic EDD observed in the current study. Adiponectin has previously been shown to enhance EDD responses to acetylcholine in healthy blood vessels. This study by Du et. al. [62], demonstrated that adiponectin signaling, through adiponectin receptor 1 on vascular endothelial cells, mediated eNOS phosphorylation and production of $^{\bullet}NO$, in a caveolin-1 dependent manner. In the current study, HMW adiponectin released from OZR-Ex tPVAT was detected at a similar level to the concentration used in the Du et. al. [62], study to induce eNOS phosphorylation (4 μg/ml vs. 5 μg/ml respectively). These data suggest that the release of HMW adiponectin from Ex tPVAT contributed to the enhanced EDD, via increased $^{\bullet}NO$ production. Conversely, TSP-1 has been shown to inhibit the activation of eNOS and reduce the production of $^{\bullet}NO$ [63]. Indeed, we observed a reduction in the levels of TSP-1 following Ex training in the OZR-Ex group, which could have contributed to the increased levels of $^{\bullet}NO$. Taken all together, these data suggest tPVAT function and cytokine profile significantly impacted aortic endothelial function and that Ex induced improvements in tPVAT phenotype that correspondingly improved aortic EDD.

Indeed, we have previously shown that a healthy (LZR) aorta was not protected against the OZR tPVAT activation of aortic $O_2^{\bullet-}$, in that LZR aortic EDD was reduced by ~ 25% in the presence of OZR tPVAT, with a corresponding reduction in $^{\bullet}NO$ production [4]. Conversely, exposing the unhealthy (OZR) aorta with LZR tPVAT lowered $O_2^{\bullet-}$ and improved $^{\bullet}NO$ production, and improved EDD in the OZR aorta by ~ 20% [4]. Further support for this idea comes from our crossover experiments in the current study, which demonstrated the OZR-Ex aorta was not protected against the inflammatory and oxidative insult released from OZR-tPVAT, and proteasome inhibition of OZR-Ex tPVAT impaired healthy donor aortic EDD. Interestingly, crossover experiments exposing OZR-Ex aorta to LZR-control tPVAT improved EDD to a similar extent as OZR-Ex aorta exposed to its own tPVAT. Furthermore, these data suggest that the tPVAT plays an important role in modulating aortic function in obesity, and following Ex, the improved aortic function was, in part, dependent on reduction of inflammatory cytokine release and proteasome function improvement in tPVAT (highlighted in Figs. 3 and 4). On a cautionary note, it was recently shown that Ex can result in very distinct adipose tissue depot-specific adaptations, i.e., the various adipose tissue depots responded quite differently to the Ex stimulus [64]. Thus, future research should further explore how the PVAT around the aorta is affected by Ex compared to other tissue depots.

To date, only two other studies have examined the effect of Ex on PVAT regulation of vascular function. In the previous studies, no effect of Ex on tPVAT mediated EDD were found in healthy rats [65], or in a rat model of diet induced obesity [66]. One potential reason for the different results is that the current study incorporated a vertical work component utilizing a 5% incline compared to 0%. In the diet induced obesity study [66], obesity did not impair the tPVAT-aorta relaxation relationship, therefore the effects of Ex in preventing or reversing disease mediated tPVAT dysfunction could not be evaluated and further highlights the novelty in the present data.

#### 4.2.3. Limitations

The current study is not without its limitations. One limitation reflects the introduction of Ex during the development of MetS. Thus, these data should be interpreted as such, and future studies to determine the therapeutic efficacy of Ex after the development of MetS on tPVAT function and regulation of aortic EDD. However, we have previously shown that at 9 weeks of age the OZR already exhibits some vascular impairment and alterations in circulating cytokines [67]. Thus, our data may reflect a halt in the progression of MetS induced aortic pathology, and a reversal in the impairments present at 9 weeks of age. Additionally, small numbers were utilized in gene expression experiments due to limited LZR tPVAT quantity. However, many genes showed robust and consistent responses such as uncoupling protein-1 and TNF. In addition, only global SOD activity was measured and data may not reflect regional alterations in specific isoforms. We recognize the inherent flaws associated with DHE imaging, however, appropriate controls measures were taken. Furthermore, we verified the elevated ROS production of the tPVAT and treated aortic lysates by the CBA assay and observed similar results. Another limitation to this study is the use of an ex-vivo approach (wire myography) to examine the interaction between tPVAT and aortic function. Although, wire myography provides a well-controlled and detailed approach to understand the physiological, pharmacological, and active biomechanical properties of blood vessels it does however have its limitations. Notably the crosstalk between endothelium and blood flow and between adventitia and adjacent tissue are disturbed under ex-vivo conditions. Furthermore, hormones, inflammatory and neural transmitters, and mechanical interactions are difficult to mimic in an ex-vivo system. As such, the ex-vivo measurements reflect the general function of the endothelium and smooth muscle without the additional effects of the systemic circulation. Future studies should examine how modulating tPVAT phenotype (via Ex, or diseases states) impacts aortic health and function in an intact system (i.e., using non-invasive imaging techniques). Lastly, for logistical reasons the current study only examined male rats. Sex steroids play an essential role in the production and function of fat and a recent study in a porcine model noted that the regulation of coronary artery tone by PVAT differed by sex [68]. Whereby, PVAT from female pigs produced an anti-contractile, relaxation response, that was not evident in PVAT from male pigs. We have previously shown that aortic EDD was similar in lean male and female rats [69], however with obesity the female OZR had a great aortic EDD than OZR male [70]. To date, it is unknown if the interplay between the aorta and tPVAT differs by sex. However, to affectively examine the potential role of sex-mediated effects, one must examine the 3 stages of the estrous cycle due to the drastic change in ovarian steroids. Future research is needed to explore the role of sex on mediating tPVAT aortic function.

## 5. Conclusions and prospective

Fig. 6 provides a summary of the main findings. The present study is the first examination of the Ex effect on tPVAT and its regulation of aortic function in MetS. Ex prevented the increase in oxidant load and inflammation associated with MetS, while enhancing $^{\bullet}NO$ and proteasome function in tPVAT. The improved tPVAT cytokine profile and proteasome function following Ex promoted aortic $^{\bullet}NO$ and EDD and our data further suggested these changes were important in the aortic

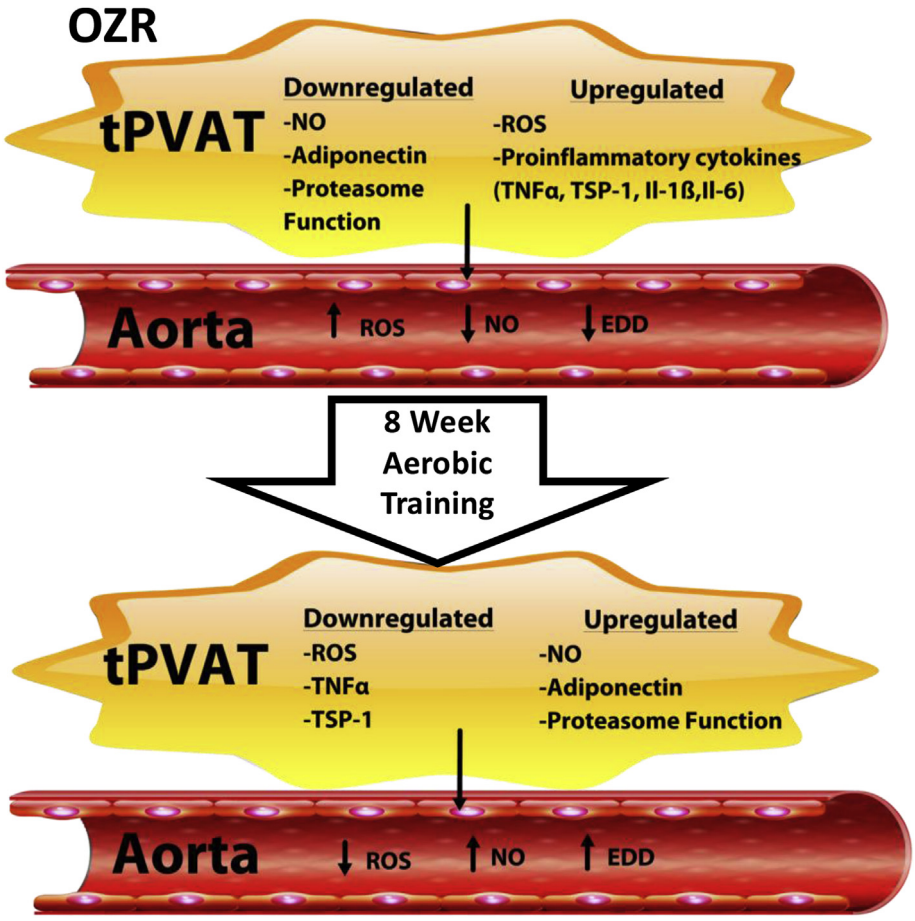


**Fig. 6. Summary of main findings from the study.**

adaptations to Ex. This was supported by the impairment of OZR-Ex aortic EDD treated with OZR tPVAT, and OZR-Ex tPVAT pretreated with a proteasome inhibitor which impaired healthy donor aortic EDD. Thus, we suggest that the tPVAT adaptation to Ex as a potential mechanism promoting cardiovascular benefits, and therapeutically targeting tPVAT in combination with Ex or other vascular therapeutics might accelerate beneficial vascular adaptation and reduce cardiovascular burden.

## Funding

This study was supported by the American Heart Association grants IRG14330015, pre-doctoral fellowship AHA (14PRE20380386); National Institute of General Medical Sciences of the National Institutes of Health (PDC and EEK; U54GM104942, and 5P20GM109098).

## Conflicts of interest

There are no conflicts of interest with this study.

## Author contributions

The study was performed in PDC laboratory. PDC, EV, KWB, RWB, JCF: Conceptualized and designed the study; PDC, EV, KWB, RA, KLM undertook experiments and analyzed data; DMS, IMO, EE, and RWB provided clinical insight and all authors critically reviewed the manuscript and approved the final manuscript as submitted and agree to be accountable for all aspects of the work.

## Appendix A. Supplementary data

Supplementary data to this article can be found online at https://doi.org/10.1016/j.redox.2019.101285.

## References

[1] E.J. Benjamin, P. Muntner, A. Alonso, M.S. Bittencourt, C.W. Callaway, A.P. Carson, A.M. Chamberlain, A.R. Chang, S. Cheng, S.R. Das, F.N. Delling, L. Djousse, M.S.V. Elkind, J.F. Ferguson, M. Fornage, L.C. Jordan, S.S. Khan, B.M. Kissela, K.L. Knutson, T.W. Kwan, D.T. Lackland, T.T. Lewis, J.H. Lichtman, C.T. Longenecker, M.S. Loop, P.L. Lutsey, S.S. Martin, K. Matsushita, A.E. Moran, M.E. Mussolino, M. O'Flaherty, A. Pandey, A.M. Perak, W.D. Rosamond, G.A. Roth, U.K.A. Sampson, G.M. Satou, E.B. Schroeder, S.H. Shah, N.L. Spartano, A. Stokes, D.L. Tirschwell, C.W. Tsao, M.P. Turakhia, L.B. VanWagner, J.T. Wilkins, S.S. Wong, S.S. Virani, E. American Heart Association Council on, C. Prevention Statistics, S. Stroke Statistics, Heart disease and stroke statistics-2019 update: a report from the American Heart association, Circulation 139 (10) (2019 Mar 5) e56.
[2] S.M. Grundy, J.I. Cleeman, S.R. Daniels, K.A. Donato, R.H. Eckel, B.A. Franklin, D.J. Gordon, R.M. Krauss, P.J. Savage, S.C. Smith Jr., J.A. Spertus, F. Costa, Diagnosis and management of the metabolic syndrome: an American Heart association/national Heart, lung, and blood Institute scientific statement, Curr. Opin. Cardiol. 21 (1) (2006) 1–6.
[3] E.S. Ford, Risks for all-cause mortality, cardiovascular disease, and diabetes associated with the metabolic syndrome: a summary of the evidence, Diabetes Care 28 (7) (2005) 1769–1778.
[4] E. DeVallance, K.W. Branyan, K. Lemaster, I.M. Olfert, D.M. Smith, E.E. Pistilli, J.C. Frisbee, P.D. Chantler, Aortic dysfunction in metabolic syndrome mediated by perivascular adipose tissue TNFalpha and NOX2 dependent pathway, Exp. Physiol. 103 (4) (2018 Apr 1) 590–603.
[5] Y.J. Gao, Z.H. Zeng, K. Teoh, A.M. Sharma, L. Abouzahr, I. Cybulsky, A. Lamy, L. Semelhago, R.M. Lee, Perivascular adipose tissue modulates vascular function in the human internal thoracic artery, J. Thorac. Cardiovasc. Surg. 130 (4) (2005) 1130–1136.
[6] X. Wang, J. Yen, P. Kaiser, L. Huang, Regulation of the 26S proteasome complex during oxidative stress, Sci. Signal. 3 (151) (2010) ra88.
[7] A.K. Ghosh, S.K. Garg, T. Mau, M. O'Brien, J. Liu, R. Yung, Elevated endoplasmic

reticulum stress response contributes to adipose tissue inflammation in aging, J Gerontol A Biol Sci Med Sci 70 (11) (2015) 1320–1329.
[8] A. Hohn, J. Konig, T. Jung, Metabolic syndrome, redox state, and the proteasomal system, Antioxidants Redox Signal. 25 (16) (2016) 902–917.
[9] T. Otoda, T. Takamura, H. Misu, T. Ota, S. Murata, H. Hayashi, H. Takayama, A. Kikuchi, T. Kanamori, K.R. Shima, F. Lan, T. Takeda, S. Kurita, K. Ishikura, Y. Kita, K. Iwayama, K. Kato, M. Uno, Y. Takeshita, M. Yamamoto, K. Tokuyama, S. Iseki, K. Tanaka, S. Kaneko, Proteasome dysfunction mediates obesity-induced endoplasmic reticulum stress and insulin resistance in the liver, Diabetes 62 (3) (2013) 811–824.
[10] V.A. Cornelissen, R.H. Fagard, Effects of endurance training on blood pressure, blood pressure-regulating mechanisms, and cardiovascular risk factors, Hypertension 46 (4) (2005) 667–675.
[11] T.D. Miller, G.J. Balady, G.F. Fletcher, Exercise and its role in the prevention and rehabilitation of cardiovascular disease, Ann. Behav. Med. 19 (3) (1997) 220–229.
[12] S.N. Blair, H.W. Kohl 3rd, C.E. Barlow, R.S. Paffenbarger Jr., L.W. Gibbons, C.A. Macera, Changes in physical fitness and all-cause mortality. A prospective study of healthy and unhealthy men, J. Am. Med. Assoc. 273 (14) (1995) 1093–1098.
[13] T. You, N.C. Arsenis, B.L. Disanzo, M.J. Lamonte, Effects of exercise training on chronic inflammation in obesity : current evidence and potential mechanisms, Sport. Med. 43 (4) (2013) 243–256.
[14] H. Nojima, H. Watanabe, K. Yamane, Y. Kitahara, K. Sekikawa, H. Yamamoto, A. Yokoyama, T. Inamizu, T. Asahara, N. Kohno, G. Hiroshima University Health Promotion Study, Effect of aerobic exercise training on oxidative stress in patients with type 2 diabetes mellitus, Metabolism 57 (2) (2008) 170–176.
[15] R. Hambrecht, V. Adams, S. Erbs, A. Linke, N. Krankel, Y. Shu, Y. Baither, S. Gielen, H. Thiele, J.F. Gummert, F.W. Mohr, G. Schuler, Regular physical activity improves endothelial function in patients with coronary artery disease by increasing phosphorylation of endothelial nitric oxide synthase, Circulation 107 (25) (2003) 3152–3158.
[16] G. Kojda, Y.C. Cheng, J. Burchfield, D.G. Harrison, Dysfunctional regulation of endothelial nitric oxide synthase (eNOS) expression in response to exercise in mice lacking one eNOS gene, Circulation 103 (23) (2001) 2839–2844.
[17] A.L. Sindler, M.D. Delp, R. Reyes, G. Wu, J.M. Muller-Delp, Effects of ageing and exercise training on eNOS uncoupling in skeletal muscle resistance arterioles, J. Physiol. 587 (Pt 15) (2009) 3885–3897.
[18] J.R. Durrant, D.R. Seals, M.L. Connell, M.J. Russell, B.R. Lawson, B.J. Folian, A.J. Donato, L.A. Lesniewski, Voluntary wheel running restores endothelial function in conduit arteries of old mice: direct evidence for reduced oxidative stress, increased superoxide dismutase activity and down-regulation of NADPH oxidase, J. Physiol. 587 (Pt 13) (2009) 3271–3285.
[19] D.A. Donley, S.B. Fournier, B.L. Reger, E. DeVallance, D.E. Bonner, I.M. Olfert, J.C. Frisbee, P.D. Chantler, Aerobic exercise training reduces arterial stiffness in metabolic syndrome, J. Appl. Physiol. 116 (11) (1985) 1396–1404 2014.
[20] T.F. Cunha, J.B. Moreira, N.A. Paixao, J.C. Campos, A.W. Monteiro, A.V. Bacurau, C.R. Bueno Jr., J.C. Ferreira, P.C. Brum, Aerobic exercise training upregulates skeletal muscle calpain and ubiquitin-proteasome systems in healthy mice, J. Appl. Physiol. 112 (11) (2012) 1839–1846.
[21] J. Zielonka, B. Kalyanaraman, Hydroethidine- and MitoSOX-derived red fluorescence is not a reliable indicator of intracellular superoxide formation: another inconvenient truth, Free Radic. Biol. Med. 48 (8) (2010) 983–1001.
[22] J. Zielonka, G. Cheng, M. Zielonka, T. Ganesh, A. Sun, J. Joseph, R. Michalski, W.J. O'Brien, J.D. Lambeth, B. Kalyanaraman, High-throughput assays for superoxide and hydrogen peroxide: design of a screening workflow to identify inhibitors of NADPH oxidases, J. Biol. Chem. 289 (23) (2014) 16176–16189.
[23] K. Martinez-Fonts, A. Matouschek, A rapid and versatile method for generating proteins with defined ubiquitin chains, Biochemistry 55 (12) (2016) 1898–1908.
[24] N.K. Brown, Z. Zhou, J. Zhang, R. Zeng, J. Wu, D.T. Eitzman, Y.E. Chen, L. Chang, Perivascular adipose tissue in vascular function and disease: a review of current research and animal models, Arterioscler. Thromb. Vasc. Biol. 34 (8) (2014) 1621–1630.
[25] Y. Lin, A.H. Berg, P. Iyengar, T.K. Lam, A. Giacca, T.P. Combs, M.W. Rajala, X. Du, B. Rollman, W. Li, M. Hawkins, N. Barzilai, C.J. Rhodes, I.G. Fantus, M. Brownlee, P.E. Scherer, The hyperglycemia-induced inflammatory response in adipocytes: the role of reactive oxygen species, J. Biol. Chem. 280 (6) (2005) 4617–4626.
[26] T. Sakamoto, N. Takahashi, Y. Sawaragi, S. Naknukool, R. Yu, T. Goto, T. Kawada, Inflammation induced by RAW macrophages suppresses UCP1 mRNA induction via ERK activation in 10T1/2 adipocytes, Am. J. Physiol. Cell Physiol. 304 (8) (2013) C729–C738.
[27] N. Xia, S. Horke, A. Habermeier, E.I. Closs, G. Reifenberg, A. Gericke, Y. Mikhed, T. Munzel, A. Daiber, U. Forstermann, H. Li, Uncoupling of endothelial nitric oxide synthase in perivascular adipose tissue of diet-induced obese mice, Arterioscler. Thromb. Vasc. Biol. 36 (1) (2016) 78–85.
[28] P. Bostrom, J. Wu, M.P. Jedrychowski, A. Korde, L. Ye, J.C. Lo, K.A. Rasbach, E.A. Bostrom, J.H. Choi, J.Z. Long, S. Kajimura, M.C. Zingaretti, B.F. Vind, H. Tu, S. Cinti, K. Hojlund, S.P. Gygi, B.M. Spiegelman, A PGC1-alpha-dependent myokine that drives brown-fat-like development of white fat and thermogenesis, Nature 481 (7382) (2012) 463–468.
[29] E. Trevellin, M. Scorzeto, M. Olivieri, M. Granzotto, A. Valerio, L. Tedesco, R. Fabris, R. Serra, M. Quarta, C. Reggiani, E. Nisoli, R. Vettor, Exercise training induces mitochondrial biogenesis and glucose uptake in subcutaneous adipose tissue through eNOS-dependent mechanisms, Diabetes 63 (8) (2014) 2800–2811.
[30] E.H. Koh, M. Kim, K.C. Ranjan, H.S. Kim, H.S. Park, K.S. Oh, I.S. Park, W.J. Lee, M.S. Kim, J.Y. Park, J.H. Youn, K.U. Lee, eNOS plays a major role in adiponectin synthesis in adipocytes, Am. J. Physiol. Endocrinol. Metab. 298 (4) (2010) E846–E853.
[31] K.I. Stanford, L.J. Goodyear, Exercise regulation of adipose tissue, Adipocyte 5 (2) (2016) 153–162.
[32] W. van Marken Lichtenbelt, Brown adipose tissue and the regulation of non-shivering thermogenesis, Curr. Opin. Clin. Nutr. Metab. Care 15 (6) (2012) 547–552.
[33] R.F. Ranallo, E.C. Rhodes, Lipid metabolism during exercise, Sport. Med. 26 (1) (1998) 29–42.
[34] K. Bedard, K.H. Krause, The NOX family of ROS-generating NADPH oxidases: physiology and pathophysiology, Physiol. Rev. 87 (1) (2007) 245–313.
[35] N. Kawanishi, H. Yano, Y. Yokogawa, K. Suzuki, Exercise training inhibits inflammation in adipose tissue via both suppression of macrophage infiltration and acceleration of phenotypic switching from M1 to M2 macrophages in high-fat-diet-induced obese mice, Exerc. Immunol. Rev. 16 (2010) 105–118.
[36] A.G. Oliveira, T.G. Araujo, B.M. Carvalho, D. Guadagnini, G.Z. Rocha, R.A. Bagarolli, J.B. Carvalheira, M.J. Saad, Acute exercise induces a phenotypic switch in adipose tissue macrophage polarization in diet-induced obese rats, Obesity 21 (12) (2013) 2545–2556.
[37] A. Ehlinger, K.J. Walters, Structural insights into proteasome activation by the 19S regulatory particle, Biochemistry 52 (21) (2013) 3618–3628.
[38] J. Rabl, D.M. Smith, Y. Yu, S.C. Chang, A.L. Goldberg, Y. Cheng, Mechanism of gate opening in the 20S proteasome by the proteasomal ATPases, Mol. Cell 30 (3) (2008) 360–368.
[39] V. Bourlier, A. Zakaroff-Girard, A. Miranville, S. De Barros, M. Maumus, C. Sengenes, J. Galitzky, M. Lafontan, F. Karpe, K.N. Frayn, A. Bouloumie, Remodeling phenotype of human subcutaneous adipose tissue macrophages, Circulation 117 (6) (2008) 806–815.
[40] C.A. Curat, V. Wegner, C. Sengenes, A. Miranville, C. Tonus, R. Busse, A. Bouloumie, Macrophages in human visceral adipose tissue: increased accumulation in obesity and a source of resistin and visfatin, Diabetologia 49 (4) (2006) 744–747.
[41] C.N. Lumeng, J.L. Bodzin, A.R. Saltiel, Obesity induces a phenotypic switch in adipose tissue macrophage polarization, J. Clin. Investig. 117 (1) (2007) 175–184.
[42] M.E. Rausch, S. Weisberg, P. Vardhana, D.V. Tortoriello, Obesity in C57BL/6J mice is characterized by adipose tissue hypoxia and cytotoxic T-cell infiltration, Int. J. Obes. 32 (3) (2008) 451–463.
[43] H. Wu, S. Ghosh, X.D. Perrard, L. Feng, G.E. Garcia, J.L. Perrard, J.F. Sweeney, L.E. Peterson, L. Chan, C.W. Smith, C.M. Ballantyne, T-cell accumulation and regulated on activation, normal T cell expressed and secreted upregulation in adipose tissue in obesity, Circulation 115 (8) (2007) 1029–1038.
[44] D. Patsouris, P.P. Li, D. Thapar, J. Chapman, J.M. Olefsky, J.G. Neels, Ablation of CD11c-positive cells normalizes insulin sensitivity in obese insulin resistant animals, Cell Metabol. 8 (4) (2008) 301–309.
[45] S. Nishimura, I. Manabe, M. Nagasaki, K. Eto, H. Yamashita, M. Ohsugi, M. Otsu, K. Hara, K. Ueki, S. Sugiura, K. Yoshimura, T. Kadowaki, R. Nagai, CD8+ effector T cells contribute to macrophage recruitment and adipose tissue inflammation in obesity, Nat. Med. 15 (8) (2009) 914–920.
[46] N. Kawanishi, T. Mizokami, H. Yano, K. Suzuki, Exercise attenuates M1 macrophages and CD8+ T cells in the adipose tissue of obese mice, Med. Sci. Sport. Exerc. 45 (9) (2013) 1684–1693.
[47] G. Gloire, S. Legrand-Poels, J. Piette, NF-kappaB activation by reactive oxygen species: fifteen years later, Biochem. Pharmacol. 72 (11) (2006) 1493–1505.
[48] S.M. Zemse, C.W. Chiao, R.H. Hilgers, R.C. Webb, Interleukin-10 inhibits the in vivo and in vitro adverse effects of TNF-alpha on the endothelium of murine aorta, Am. J. Physiol. Heart Circ. Physiol. 299 (4) (2010) H1160–H1167.
[49] M. Kamizato, K. Nishida, K. Masuda, K. Takeo, Y. Yamamoto, T. Kawai, S. Teshima-Kondo, T. Tanahashi, K. Rokutan, Interleukin 10 inhibits interferon gamma- and tumor necrosis factor alpha-stimulated activation of NADPH oxidase 1 in human colonic epithelial cells and the mouse colon, J. Gastroenterol. 44 (12) (2009) 1172–1184.
[50] Z.V. Wang, P.E. Scherer, Adiponectin, cardiovascular function, and hypertension, Hypertension 51 (1) (2008) 8–14.
[51] J.S. Isenberg, G. Martin-Manso, J.B. Maxhimer, D.D. Roberts, Regulation of nitric oxide signalling by thrombospondin 1: implications for anti-angiogenic therapies, Nat. Rev. Cancer 9 (3) (2009) 182–194.
[52] W.K. Mandler, T.R. Nurkiewicz, D.W. Porter, I.M. Olfert, Thrombospondin-1 mediates multi-walled carbon nanotube induced impairment of arteriolar dilation, Nanotoxicology 11 (1) (2017) 112–122.
[53] R.W. O'Rourke, A.E. White, M.D. Metcalf, A.S. Olivas, P. Mitra, W.G. Larison, E.C. Cheang, O. Varlamov, C.L. Corless, C.T. Roberts Jr., D.L. Marks, Hypoxia-induced inflammatory cytokine secretion in human adipose tissue stromovascular cells, Diabetologia 54 (6) (2011) 1480–1490.
[54] S.P. Didion, D.A. Kinzenbaw, L.I. Schrader, Y. Chu, F.M. Faraci, Endogenous interleukin-10 inhibits angiotensin II-induced vascular dysfunction, Hypertension 54 (3) (2009) 619–624.
[55] P.A. VanderLaan, C.A. Reardon, G.S. Getz, Site specificity of atherosclerosis: site-selective responses to atherosclerotic modulators, Arterioscler. Thromb. Vasc. Biol. 24 (1) (2004) 12–22.
[56] J. Padilla, G.H. Simmons, S.B. Bender, A.A. Arce-Esquivel, J.J. Whyte, M.H. Laughlin, Vascular effects of exercise: endothelial adaptations beyond active muscle beds, Physiology 26 (3) (2011) 132–145.
[57] D.J. Green, M.T. Hopman, J. Padilla, M.H. Laughlin, D.H. Thijssen, Vascular adaptation to exercise in humans: role of hemodynamic stimuli, Physiol. Rev. 97 (2) (2017) 495–528.
[58] J.W. Rush, J.R. Turk, M.H. Laughlin, Exercise training regulates SOD-1 and oxidative stress in porcine aortic endothelium, Am. J. Physiol. Heart Circ. Physiol. 284

(4) (2003) H1378–H1387.
[59] G.H. Simmons, J. Padilla, M.H. Laughlin, Heterogeneity of endothelial cell phenotype within and amongst conduit vessels of the swine vasculature, Exp. Physiol. 97 (9) (2012) 1074–1082.
[60] J. Padilla, N.T. Jenkins, V.J. Vieira-Potter, M.H. Laughlin, Divergent phenotype of rat thoracic and abdominal perivascular adipose tissues, Am. J. Physiol. Regul. Integr. Comp. Physiol. 304 (7) (2013) R543–R552.
[61] B. Yang, V. Rizzo, TNF-alpha potentiates protein-tyrosine nitration through activation of NADPH oxidase and eNOS localized in membrane rafts and caveolae of bovine aortic endothelial cells, Am. J. Physiol. Heart Circ. Physiol. 292 (2) (2007) H954–H962.
[62] Y. Du, R. Li, W.B. Lau, J. Zhao, B. Lopez, T.A. Christopher, X.L. Ma, Y. Wang, Adiponectin at physiologically relevant concentrations enhances the vasorelaxative effect of acetylcholine via cav-1/AdipoR-1 signaling, PLoS One 11 (3) (2016) e0152247.
[63] E.M. Bauer, Y. Qin, T.W. Miller, R.W. Bandle, G. Csanyi, P.J. Pagano, P.M. Bauer, J. Schnermann, D.D. Roberts, J.S. Isenberg, Thrombospondin-1 supports blood pressure by limiting eNOS activation and endothelial-dependent vasorelaxation, Cardiovasc. Res. 88 (3) (2010) 471–481.
[64] A.C. Lehnig, R.S. Dewal, L.A. Baer, K.M. Kitching, V.R. Munoz, P.J. Arts, D.A. Sindeldecker, F.J. May, H. Lauritzen, L.J. Goodyear, K.I. Stanford, Exercise training induces depot-specific adaptations to white and Brown adipose tissue, iScience 11 (2019) 425–439.
[65] H.N. Araujo, C.P. Valgas da Silva, A.C. Sponton, S.P. Clerici, A.P. Davel, E. Antunes, A. Zanesco, M.A. Delbin, Perivascular adipose tissue and vascular responses in healthy trained rats, Life Sci. 125 (2015) 79–87.
[66] H.N. Araujo, J.A. Victorio, C.P. Valgas da Silva, A.C.S. Sponton, J.F. Vettorazzi, C. de Moraes, A.P. Davel, A. Zanesco, M.A. Delbin, Anti-contractile effects of perivascular adipose tissue in thoracic aorta from rats fed a high-fat diet: role of aerobic exercise training, Clin. Exp. Pharmacol. Physiol. 45 (3) (2018) 293–302.
[67] S.D. Brooks, E. DeVallance, A.C. d'Audiffret, S.J. Frisbee, L.E. Tabone, C.D. Shrader, J.C. Frisbee, P.D. Chantler, Metabolic syndrome impairs reactivity and wall mechanics of cerebral resistance arteries in obese Zucker rats, Am. J. Physiol. Heart Circ. Physiol. 309 (11) (2015) H1846–H1859.
[68] A.A. Ahmad, M.D. Randall, R.E. Roberts, Sex differences in the regulation of porcine coronary artery tone by perivascular adipose tissue: a role of adiponectin? Br. J. Pharmacol. 174 (16) (2017) 2773–2783.
[69] S.D. Brooks, S. Hileman, P.D. Chantler, S. Milde, K.C. Lemaster, S. Frisbee, J.K. Shoemaker, D.N. Jackson, J.C. Frisbee, Protection from vascular dysfunction in female rats with chronic stress and depressive symptoms, Am. J. Physiol. Heart Circ. Physiol. 314 (5) (2018 May 1) H1070–H1084.
[70] S.D. Brooks, S. Hileman, P.D. Chantler, S. Milde, K.C. Lemaster, S. Frisbee, J.K. Shoemaker, D.N. Jackson, J.C. Frisbee, Protection from chronic stress- and depressive symptom-induced vascular endothelial dysfunction in female rats is abolished by pre-existing metabolic disease, Am. J. Physiol. Heart Circ. Physiol. 314 (5) (2018 May 1) H1085–H1097.